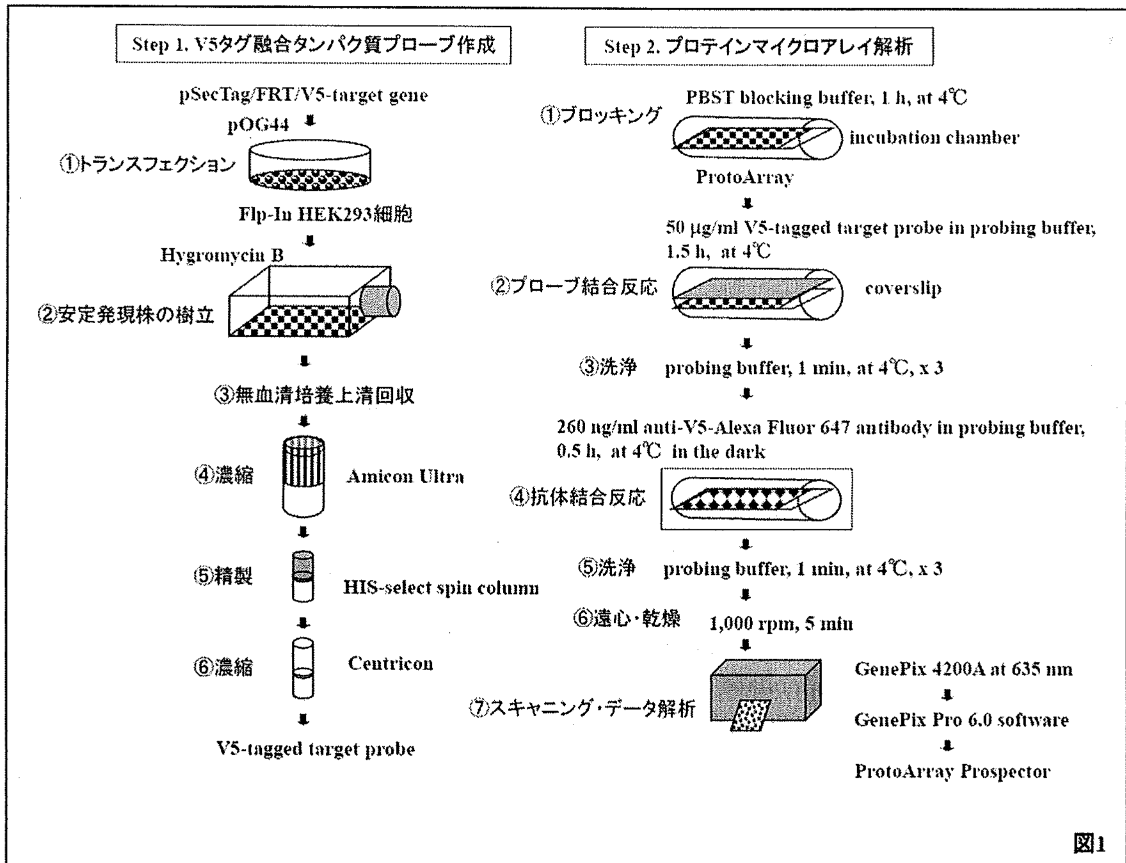

図 1. プロトアレイによるタンパク質間相互作用の解析.
目的タンパク質のV5タグ融合タンパク質プローブを作成し(step 1)、プロテインマイクロアレイ(ProtoArray)と反応させ、蛍光シグナルをスキャナーで検出する(step 2)。詳細は本文参照。図は論文(3)より引用改変。

Neuropathology and Applied Neurobiology (2009), **35**, 16–35 doi: 10.1111/j.1365-2990.2008.00947.x

Protein microarray analysis identifies human cellular prion protein interactors

J. Satoh*†, S. Obayashi*, T. Misawa*, K. Sumiyoshi*, K. Oosumi* and H. Tabunoki*

**Department of Bioinformatics and Molecular Neuropathology, Meiji Pharmaceutical University, and †Department of Immunology, National Institute of Neuroscience, NCNP, Tokyo, Japan*

J. Satoh, S. Obayashi, T. Misawa, K. Sumiyoshi, K. Oosumi and H. Tabunoki (2009) *Neuropathology and Applied Neurobiology* 35, 16–35

Protein microarray analysis identifies human cellular prion protein interactors

Aims: To obtain an insight into the function of cellular prion protein (PrPC), we studied PrPC-interacting proteins (PrPIPs) by analysing a protein microarray. **Methods:** We identified 47 novel PrPIPs by probing an array of 5000 human proteins with recombinant human PrPC spanning amino acid residues 23–231 named PR209. **Results:** The great majority of 47 PrPIPs were annotated as proteins involved in the recognition of nucleic acids. Coimmunoprecipitation and cell imaging in a transient expression system validated the interaction of PR209 with neuronal PrPIPs, such as FAM64A, HOXA1, PLK3 and MPG. However, the interaction did not generate proteinase K-resistant proteins. KeyMolnet, a bioinformatics tool for analysing molecular interaction on the curated knowledge database, revealed that the complex molecular network of PrPC and PrPIPs has a significant relationship with AKT, JNK and MAPK signalling pathways. **Conclusions:** Protein microarray is a useful tool for systematic screening and comprehensive profiling of the human PrPC interactome. Because the network of PrPC and interactors involves signalling pathways essential for regulation of cell survival, differentiation, proliferation and apoptosis, these observations suggest a logical hypothesis that dysregulation of the PrPC interactome might induce extensive neurodegeneration in prion diseases.

Keywords: cellular prion protein, KeyMolnet, protein microarray, protein–protein interaction

Published online *Article Accepted* on 23th February 2008

Introduction

Prion diseases are a group of neurodegenerative disorders affecting both animals and humans [1,2]. The great majority of prion diseases are transmissible, and characterized by intracerebral accumulation of an abnormal prion protein (PrPSc) that is identical in amino acid sequence to the cellular isoform (PrPC) encoded by the *PRNP* gene. PrPC is expressed widely in neural and non-neural tissues at the highest level in neurones in the central nervous system (CNS) [3]. PrPSc differs biochemically from PrPC by its β sheet-enriched structure, detergent insolubility, limited proteolysis by proteinase K, a slower turnover rate and infectivity. Previous studies suggested that the protein conformational conversion of α-helix-rich PrPC into β sheet-rich PrPSc involves a homotypic interaction between endogenous PrPC and incoming or *de novo* generated PrPSc via a post-translational process mediated by as yet unidentified species-specific auxiliary factor(s) named 'protein X' [4,5].

At present, the biological function of PrPC remains largely unknown. Several lines of PrPC-deficient mice were established independently by different gene-targeting strategies [6–8]. All of them exhibited normal early development and complete protection against scrapie infection. These observations indicate that PrPC is dispensable for embryonic development, but is pivotal for inducing prion

Correspondence: Jun-ichi Satoh, Department of Bioinformatics and Molecular Neuropathology, Meiji Pharmaceutical University, 2-522-1 Noshio, Kiyose, Tokyo 204-8588, Japan. Tel: +81 42 4958678; Fax: +81 42 4958678; E-mail: satoj@my-pharm.ac.jp

© 2008 Blackwell Publishing Ltd

diseases. Several *in vitro* studies suggested a role of PrPC in neuritogenesis [9,10], neuronal cell adhesion [11] and a receptor for neurotrophic factors [12]. More consistently, many studies indicated that an octapeptide repeat region of PrPC with a copper-binding capacity exhibits an antioxidant activity [13]. However, none of previous findings provided an adequate explanation for mild phenotypes of PrPC-deficient mice.

A number of previous studies, by employing mainly the yeast two-hybrid (Y2H) screening system, identified a wide variety of PrPC-interacting proteins (PrPIPs). They include synapsin I [14], glial fibrillary acidic protein [15], amyloid precursor-like protein 1 [16], heat shock protein Hsp60 [17–19], the Hsp cofactor STI-1 [20], the antiapoptotic molecule Bcl-2 [21], signal-transducing adapters such as Grb2 [14], ZAP70 [22] and 14-3-3 [23], neurotrophin receptor interacting MAGE homolog [24], tubulin [25], heterogeneous ribonuclear protein A2/B1 [26], casein kinase 2 [27], plasminogen [28], laminin receptor precursor [29], laminin [9] and vitronection [30]. Most of these molecules play a key role in signal-transducing events essential for neuronal function. However, none of them could serve as the chaperone 'protein X'.

The Y2H system is a powerful approach to identify novel protein–protein interactions. However, Y2H screening requires a lot of time and effort, and is often criticized for detecting the interactions unrelated to the physiological setting, and obtaining high rates of false positive interactors caused by spontaneous activation of reporter genes and self-activating bait proteins [31,32]. Recently, protein microarray technology has been established for rapid, systematic and less expensive screening of thousands of protein–protein interactions in a high-throughput fashion [33,34]. The array includes numerous protein targets of various functional classes immobilized on a single glass slide. The protein microarray has important applications in the areas not only of basic biological research on a whole-proteome scale, but also of drug discovery research of target identification [35,36].

In order to establish a therapeutic intervention targeted on prion propagation, it is essential to clarify the biological function of PrPC and the pathological implication of PrPSc, and equally important to identify all human PrPIPs, some of which potentially serve as a candidate for 'protein X'. The present study was designed to identify a comprehensive profile of the human PrPC interactome by analysing a high-density protein microarray, and to obtain an insight into the PrPC–PrPIPs network.

Materials and methods

Preparation of a V5-tagged PrP probe for microarray analysis

Human embryonic kidney cells HEK293, whose genome was modified for the Flp-In system (Flp-In 293; Invitrogen, Carlsbad, CA), contain a single Flp recombination target (FRT) site targeted for the site-specific recombination, integrated in a transcriptionally active locus of the genome, where it stably expresses the *lacZ*–Zeocin fusion gene driven from the pFRT/*lac*Zeo plasmid under the control of SV40 early promoter. The cells were maintained in Dulbecco's modified Eagle's medium supplemented with 10% foetal bovine serum, 100 U/ml penicillin and 100 μg/ml streptomycin (feeding medium) with inclusion of 100 μg/ml zeocin, as described previously [37].

To prepare the probe for protein microarray analysis, the gene encoding a truncated form of human PrPC spanning amino acid residues 23–231 named PR209 was amplified by polymerase chain reaction (PCR) using PfuTurbo DNA polymerase (Stratagene, La Jolla, CA) and the primer sets listed in Table S1 online. The PCR product was then cloned into a mammalian expression vector pSecTag/FRT/V5-His TOPO (Invitrogen) to produce a fusion protein with a C-terminal V5 tag, a C-terminal polyhistidine (6xHis) tag and an N-terminal Ig κ-chain secretion signal. This vector, together with the Flp recombinase expression vector pOG44 (Invitrogen), was transfected in Flp-In 293 cells by Lipofectamine 2000 reagent (Invitrogen). A stable cell line was established after incubating the transfected cells for 1 month in the feeding medium with inclusion of 100 μg/ml hygromycin B. In this system, the recombinant protein was secreted into the culture medium after the Ig κ-chain secretion signal sequence was processed by an endogenous signal peptidase-mediated cleavage.

To purify the V5-tagged PR209 protein, the serum-free culture supernatant was harvested, and concentrated at a 1/40 volume by centrifugation on an Amicon Ultra-15 filter (Millipore, Bedford, MA). It was then purified by the HIS-select spin column (Sigma, St. Louis, MO), and concentrated at a 1/10 volume by centrifugation on a Centricon-10 filter (Millipore). The protein concentration was determined by a Bradford assay kit (Bio-Rad, Hercules, CA). The purity and specificity of the probe were verified by Western blot analysis using mouse monoclonal anti-V5 antibody (Invitrogen), mouse monoclonal anti-

PrP antibody 3F4 (Dako, Tokyo, Japan) and rabbit polyclonal antibody C20 specific for the sequence close to the C-terminus of PrPC (Santa Cruz Biotechnology, Santa Cruz, CA). To determine the status of glycosylation, 5 μg of the probe protein was deglycosylated by incubating it at 37°C for 1.5 h with 5000 U peptide N-glycosidase F (New England BioLabs, Beverly, MA), followed by separation on the gel [37].

Protein microarray analysis

The present study utilized the ProtoArray human protein microarray v3.0 (Invitrogen). It contains approximately 5000 recombinant GST-tagged human proteins expressed by the baculovirus expression system and purified under native conditions by using gluthathione affinity chromatography to ensure the preservation of native structure, post-translational modifications and proper functionality of target proteins [36,38]. They were spotted in duplicate on a nitrocellulose-coated glass slide. The target proteins cover a wide range of biologically important proteins selected from the human ultimate open reading frame (ORF) clone collection (Invitrogen). The probe is spatially accessible to all parts of target proteins on the array, which protrude from the glass slide surface via the N-terminal GST fusion tag serving as a spacer. The complete list is shown in Table S2 online. The proteins are spotted in an arrangement of 4 × 12 subarrays equally spaced in vertical and horizontal directions. Each subarray includes 20 × 20 spots, composed of 76 positive and negative control spots (C), 222 human target proteins (H), and 102 blanks and empty spots (B) (Figure 1**b**). The 14 positive control spots include four of an Alexa Fluor 647-labelled antibody (row 1, columns 1, 2; row 14, columns 13, 14), six of a concentration gradient of a biotinylated anti-mouse antibody with a capacity to bind to mouse monoclonal anti-V5 antibody conjugated with Alexa Fluor 647 (row 14, columns 15–20), and four of a concentration gradient of V5 protein (row 15, columns 5–8). The 62 negative control spots include six of a concentration gradient of bovine serum albumin (BSA) (row 1, columns 3–8), four of a concentration gradient of a rabbit anti-GST antibody (row 1, columns 9–12), four of a concentration gradient of calmodulin (row 1, columns 13–16), 16 of a concentration gradient of GST (row 1, columns 17–20; row 2, columns 1–12), 10 of buffer only (row 15, columns 1, 2, 9–16), eight of human IgG subclasses (row 15, columns 17–20; row 16, columns 1–4), 12 of Invitrogen internal controls (row 4, columns 9, 10; row 6, columns 15–18; row 7, columns 9, 10, 15, 16; row 8, columns 13, 14), and two of an antibiotin antibody (row 15, columns 3, 4).

Non-specific binding was blocked by incubating the array for 90 min in the PBST blocking buffer composed of 1% BSA and 0.1% Tween 20 in phosphate-buffered saline (PBS). Then, it was incubated for 30 min at 4°C with the probe described above at a concentration of 200 μg/ml in the probing buffer composed of 1% BSA, 5 mM $MgCl_2$, 0.5 mM dithiothreitol, 0.05% Triton X-100 and 5% glycerol in PBS. The array was washed three times with the probing buffer, and then incubated for 30 min at 4°C with mouse monoclonal anti-V5 antibody labelled with Alexa Fluor 647 (Invitrogen) at a concentration of 260 ng/ml in the probing buffer. Then, the array was washed three times with the probing buffer, and scanned by the GenePix 4200 A scanner (Axon Instruments, Union City, CA) at a wavelength of 635 nm. The data were analysed by using the ProtoArray Prospector software v3.0 (Invitrogen), following acquisition of the microarray lot-specific information, which compensates inter-lot variations in protein concentrations identified by the post-printing quality control. According to the manufacturer-recommended setting of the ProtoArray Prospector software, the spots showing the background-subtracted signal intensity value greater than the median plus three standard deviations of all the fluorescence intensities were considered as having significant interactions. The Z-score, an indicator for statistical significance of binding specificity, was calculated as the background-subtracted signal intensity value of the target protein minus the average of the background-subtracted signal intensity value from the negative control distribution, divided by the standard deviation of the negative control distribution.

Bioinformatics analysis

The gene expression pattern of mouse orthologues of PrPIPs in the brain was searched on the Allen Brain Atlas database [39], an anatomically comprehensive digital atlas containing the expression patterns of more than 20 000 genes in the adult mouse brain analysed by high-throughput *in situ* hybridization methods (http://www.brain-map.org).

The interaction of PrPC with PrPIPs was searched on the Biomolecular Interaction Network database (BIND) (http://bond.unleashedinformatics.com). Functional

© 2008 Blackwell Publishing Ltd,

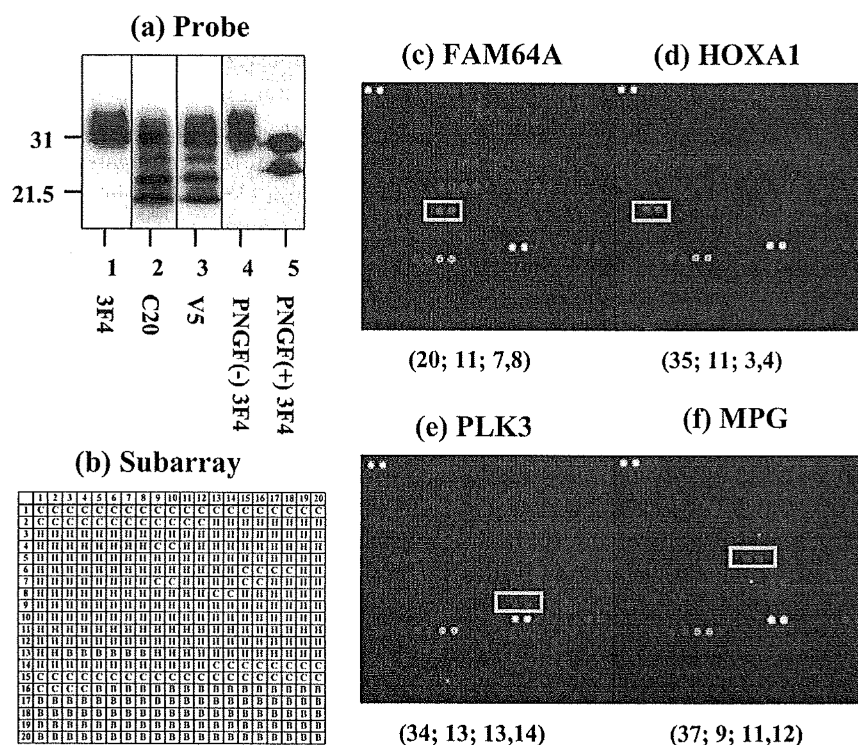

Figure 1. Protein microarray analysis. (a) Western blot of PR209 probe. The lanes (1–5) represent the immunolabelling with the antibodies following: (1) 3F4, (2) C20, (3) V5, (4) 3F4 before treatment with peptide N-glycosidase F (PNGase F) and (5) 3F4 after treatment with PNGase F. (b) The layout of subarray. The high-density protein microarray (5000 proteins, duplicate spots each) utilized in the present study contains 4 × 12 subarrays. Each subarray includes 20 × 20 spots. They are composed of 76 control spots (C) including 14 positive and 62 negative control spots, 222 human target proteins (H) and 102 blanks and empty spots (B), as described in *Materials and methods*. (c) FAM64A. The spot location is subarray 20, row 11, columns 7, 8. (d) HOXA1. Subarray 35, row 11, columns 3, 4. (e) PLK3. Subarray 34, row 13, columns 13, 14. (f) MPG. Subarray 37, row 9, columns 11, 12. PR209 interactors located on different subarrays (c–f) are indicated by an enclosed yellow line. It is worthy to note that in each subarray, positive control spots composed of an Alexa Fluor 647-labelled antibody (row 1, columns 1, 2; row 14, columns 13, 14), a concentration gradient of a biotinylated anti-mouse antibody with a capacity to bind to mouse monoclonal anti-V5 antibody conjugated with Alexa Fluor 647 (row 14, columns 15–20; signals visible on the higher concentration), and a concentration gradient of V5 protein (row 15, columns 5–8; signals visible on the higher concentration) are identified as positive, whereas negative control spots composed of a concentration gradient of BSA (row 1, columns 3–8), a concentration gradient of a rabbit anti-GST antibody (row 1, columns 9–12), a concentration gradient of calmodulin (row 1, columns 13–16), a concentration gradient of GST (row 1, columns 17–20; row 2, columns 1–12), buffer only (row 15; columns 1, 2, 9–16), human IgG subclasses (row 15, columns 17–20; row 16, columns 1–4), Invitrogen internal controls (row 4, columns 9, 10; row 6, columns 15–18; row 7, columns 9, 10, 15, 16; row 8, columns 13, 14), and an antibiotin antibody (row 15, columns 3, 4) are found as negative.

annotation of PrPIPs was searched by the web-accessible program named Database for Annotation, Visualization and Integrated Discovery (DAVID) version 2007, National Institute of Allergy and Infectious Diseases, National Institutes of Health (NIH) (http://david.abcc.ncifcrf.gov) [40]. It covers more than 40 annotation categories, including Gene Ontology terms, protein–protein interactions, protein functional domains, disease associations, biological pathways, sequence general features, homologies, gene functional summaries and tissue expressions. By importing the list of Entrez gene IDs of PrPIPs, this program creates the functional annotation chart, an annotation term-focused view that lists annotation terms and their associated genes under study. To avoid excessive counting of duplicated genes, the Fisher's exact statistics is calculated based on corresponding DAVID gene IDs by which all redundancies in original IDs are removed.

The molecular network of PrPIPs was analysed by the software named KeyMolnet (Institute of Medicinal Molecular Design, Tokyo, Japan) [41]. It operates on a comprehensive knowledge database, composed of information on relationships among human genes, molecules, diseases, pathways and drugs, carefully curated by expert biologists from review articles, literature and public

databases. They are categorized into the core contents collected from selected review articles with the highest reliability or the secondary contents extracted from abstracts of PubMed database and Human Reference Protein database.

By importing the list of Entrez gene IDs, KeyMolnet automatically provides corresponding molecules as a node on networks [41,42]. Among various network-searching algorithms, the 'N-points to N-points' search extracts the molecular network with the shortest route connecting the starting-point molecules and the end-point molecules. The generated network was compared side by side with 346 human canonical pathways of the KeyMolnet library. The algorithm counting the number of overlapping molecular relations between the extracted network and the canonical pathway makes it possible to identify the canonical pathway showing the most significant contribution to the extracted network. The significance in the similarity between both is scored following the formula, where O = the number of overlapping molecular relations between the extracted network and the canonical pathway, V = the number of molecular relations located in the extracted network, C = the number of molecular relations located in the canonical pathway, T = the number of total molecular relations (approximately 90 000 sets) and X = the sigma variable that defines incidental agreements.

$$\text{score} = -\log_2\left(\sum_{x=O}^{Min(C,V)} f(x)\right)$$

$$f(x) = {}_{C}C_{X} \cdot {}_{T\text{-}C}C_{V\text{-}x} / {}_{T}C_{V}$$

Immunoprecipitation and Western blot analysis

PR209, the N-terminal half of PR209 (amino acid residues 23–121), the C-terminal half of PR209 (amino acid residues 122–231), and the ORF of family with sequence similarity 64, member A (FAM64A), polo-like kinase 3 (PLK3), N-methylpurine-DNA glycosylase (MPG) and homeobox A1 (HOXA1) were amplified by PCR using PfuTurbo DNA polymerase and the primer sets listed in Table S1 online. They were then cloned into the mammalian expression vector p3XFLAG-CMV7.1 (Sigma) or pCMV-Myc (Clontech, Mountain View, CA) to express a fusion protein with an N-terminal Flag or Myc tag. At 48 h after co-transfection of the vectors, HEK293 cells were homogenized in M-PER lysis buffer (Pierce, Rockford, IL) supplemented with a cocktail of protease inhibitors (Sigma). In limited experiments, a proteasome inhibitor MG-132 (Merck-Calbiochem, Tokyo, Japan) was added at a final concentration of 10 μM in the culture medium during the last 24 h before harvest. After preclearance, the supernatant was incubated at 4°C for 3 h with mouse monoclonal anti-Flag M2 affinity gel (Sigma), rabbit polyclonal anti-Myc-conjugated agarose (Sigma) or the same amount of normal mouse or rabbit IgG-conjugated agarose (Santa Cruz Biotechnology). After several washes, the immunoprecipitates were processed for Western blot analysis using rabbit polyclonal anti-Myc antibody (Sigma) and mouse monoclonal anti-FLAG M2 antibody (Sigma). The specific reaction was visualized using a chemiluminescence substrate (Pierce).

To determine the proteinase K-resistant property of PR209, the cells were homogenized in M-PER lysis buffer without inclusion of protease inhibitors. The protein extract was then incubated at 37°C for 30 min with 5 μg/ml recombinant proteinase K (Roche Diagnostics, Mannheim, Germany), followed by adding phenylmethylsulphonyl fluoride at a final concentration of 5 mM, according to the methods described previously [43]. Proteins were precipitated by adding 6% trichloroacetic acid. After centrifugation at 4°C for 15 min at 16 100 g, the pellets were washed with cold acetone, and processed for Western blot analysis using 3F4 antibody.

To determine the detergent-insoluble property of PR209, the cells were homogenized in a lysis buffer containing 100 mM NaCl, 10 mM EDTA, 10 mM Tis (pH 7.4), 0.5% Nonidet P-40 and 0.5% sodium deoxycholate, according to the methods described previously [44]. The lysate was centrifuged at 4°C for 10 min at 2000 g to remove debris. Then, the supernatant was further centrifuged at 4°C for 1 h at 16 100 g to separate detergent-soluble (supernatant) and detergent-insoluble (pellet) fractions. They were processed for Western blot analysis using 3F4 antibody. HRP-conjugated secondary antibodies were obtained from Santa Cruz Biotechnology.

Cell imaging analysis

PR209 and the ORF of FAM64A, PLK3, MPG and HOXA1 were amplified by PCR using PfuTurbo DNA polymerase and the primer sets listed in Table S1 online. They were then cloned into the mammalian expression vector pDsRed-Express-C1 (Clontech), pEYFP-C1 (Clontech), pcDNA3.1/NT/GFP-TOPO (Invitrogen) or pcDNA3.1/CT/GFP-TOPO (Invitrogen) to express a fusion protein with an N-terminal or C-terminal DsRed, EYFP or GFP tag. At 24–48 h after co-transfection of the vectors, the cells were

© 2008 Blackwell Publishing Ltd,

fixed briefly in 4% paraformaldehyde, mounted on slides with glycerol-polyvinyl alcohol, and examined on the Olympus BX51 universal microscope.

Human neural cell lines and cultures

Human astrocytes (AS) in culture were established from neuronal progenitor (NP) cells of human foetal brain (Cambrex, Walkersville, MD). For the induction of neuronal differentiation, NTera2 cells maintained in the undifferentiated state (NTera2-U) were incubated for 4 weeks in feeding medium containing 10^{-5} M *all trans* retinoic acid (Sigma), replated twice and then plated on a surface coated with Matrigel Basement Membrane Matrix (Becton Dickinson, Bedford, MA). They were incubated for another 2 weeks in feeding medium containing a cocktail of mitotic inhibitors, resulting in the enrichment of differentiated neurones (NTera2-N), as described previously [45]. Human microglia cell line HMO6 was provided by Dr Seung U. Kim, Division of Neurology, University of British Columbia, Vancouver, B.C., Canada. Total RNA of the human frontal cerebral cortex was obtained from Clontech.

Reverse transcription-PCR analysis

DNase-treated total cellular RNA was processed for cDNA synthesis using oligo$(dT)_{12-18}$ primers and SuperScript II reverse transcriptase (Invitrogen). Then, cDNA was amplified by PCR using HotStar Taq DNA polymerase (Qiagen, Valencia, CA) and a panel of primer sets listed in Table S1 online. The amplification program consisted of an initial denaturing step at 95°C for 15 min, followed by a denaturing step at 94°C for 1 min, an annealing step at 60°C for 40 s and an extension step at 72.9°C for 50 s for 30–35 cycles, except for the glyceraldehyde-3-phosphate dehydrogenase (G3PDH), an internal control, amplified for 27 cycles.

Results

Protein microarray analysis identified 47 novel PrPC interactors

To analyse the human protein microarray, V5-tagged PR209 probe was purified from the supernatant of a stable cell line secreting the recombinant protein in the culture medium. By Western blot analysis, the probe was composed of a mixture of glycosylated full-length and N-terminally truncated forms of PrPC (Figure 1**a**, lanes 1–5). The 18.5-kDa protein identified by C20 but not by 3F4 represents the C-terminal fragment produced by constitutive metalloprotease-mediated cleavage [46]. Among total 5000 proteins on the array, 47 were identified as the proteins showing significant interaction with the probe (Table 1). They include FAM64A (Figure 1c), HOXA1 (Figure 1d), casein kappa (CSN3), bromodomain adjacent to zinc finger domain, 2B (BAZ2B), chromosome 7 ORF 50 (C7orf50), surfeit 2 (SURF2), sodium channel modifier 1 (SCNM1), chromosome 18 ORF 56 (C18orf56), PLK3 (Figure 1e), RNA binding motif protein 22 (RBM22), hypothetical protein DKFZp761B107, MPG (Figure 1f), zinc finger protein 192 (ZNF192), thymic stromal lymphopoietin (TSLP), DEAD box polypeptide 47 (DDX47), MAP/microtubule affinity-regulating kinase 4 (MARK4), zinc finger protein 408 (ZNF408), TBP-like 1 (TBPL1), activator of basal transcription 1 (ABT1), ribosomal protein L41 (RPL41), zinc finger protein 740 (ZNF740), CWC15 homolog, four and a half LIM domains 1 (FHL1), amyotrophic lateral sclerosis 2 chromosome region, candidate 4 (ALS2CR4), immediate early response 3 (IER3), KIAA1191, peptidyl-tRNA hydrolase 1 homolog (PTRH1), phosphodiesterase 4D interacting protein (PDE4DIP), Rho GTPase activating protein 15 (ARHGAP15), mitochondrial GTPase 1 homolog (MTG1), cirrhosis, autosomal recessive 1 A (CIRH1A), eukaryotic translation initiation factor 2C, 1 (EIF2C1), WD repeat domain 5 (WDR5), centaurin, alpha 2 (CENTA2), protein phosphatase 1, regulatory subunit 14 A (PP1R14 A), cold inducible RNA binding protein (CIRBP), zinc finger, FYVE domain containing 28 (ZFYVE28), within bgcn homolog (WIBG), nucleolar protein family A, member 2 (NOLA2), PTPRF interacting protein, binding protein 2 (PPFIBP2), family with sequence similarity 27, member E3 (FAM27E3), fibroblast growth factor 13 (FGF13), apoptosis-inducing factor, mitochondrion-associated, 3 (AIFM3), 2′,3′-cyclic nucleotide 3′ phosphodiesterase (CNP), NIN1/RPN12 binding protein 1 homolog (NOB1), RNA-binding region containing 3 (RNPC3) and dual-specificity tyrosine-phosphorylation regulated kinase 3 (DYRK3). The gene expression pattern of PrPC interactors (PrPIPs) in the adult brain analysed by *in situ* hybridization was searched on the Allen Brain Atlas database [39]. Among 47 PrPIPs, at least 35 mouse orthologues (74%) were expressed in various regions of the adult mouse brain (Table 1). The expression pattern of the remaining

Table 1. PrPC-interacting proteins (PrPIPs) identified by protein microarray analysis

No.	*Entrez gene ID*	*Gene symbol*	*Gene name*	*Putative molecular function*	*Block*	*Row*	*Column*	*Z-score*	*Gene expression in adult mouse brain (region with the highest expression level)*
1	54478	FAM64A	Family with sequence similarity 64, member A	A protein with the DUF1466 domain of unknown function	20	11	7, 8	21.89656	Unknown
2	3198	HOXA1	Homeobox A1	A transcription factor that regulates the placement of hindbrain segments in the proper location along the anterior–posterior axis during development	35	11	3, 4	18.36074	Yes (CB)
3	1448	CSN3	Casein kappa	A milk protein	20	9	9, 10	12.58106	Yes (OLF)
4	29994	BAZ2B	Bromodomain adjacent to zinc finger domain, 2B	A component of chromatin remodeling complexes	24	10	5, 6	7.96988	Yes (MY)
5	84310	C7orf50	Chromosome 7 open reading frame 50	A hypothetical protein of unknown function	21	11	9, 10	6.7938	Unknown
6	6835	SURF2	Surfeit 2	The housekeeping gene of unknown function	15	9	15, 16	6.31368	Yes (MY)
7	79005	SCNM1	Sodium channel modifier 1	A zinc finger protein acting as a premRNA splicing factor	18	6	3, 4	6.06453	Yes (CB and other regions)
8	494514	C18orf56	Chromosome 18 open reading frame 56	A hypothetical protein of unknown function	10	10	19, 20	6.02515	Unknown
9	1263	PLK3	Polo-like kinase 3 (Drosophila)	A serine/threonine kinase that regulates cell cycle progression	34	13	13, 14	5.94109	Yes (MY)
10	55696	RBM22	RNA binding motif protein 22	A zinc finger protein with the RNA recognition motif of unknown function	20	9	7, 8	5.67225	Yes (CB)
11	91050	DKFZp761B107	Hypothetical protein DKFZp761B107	A protein with the SMC N-terminal domain of unknown function	22	12	3, 4	5.36251	Unknown
12	4350	MPG	N-methylpurine-DNA glycosylase	A DNA glycosylase acting as a DNA repair enzyme	37	9	11, 12	5.16637	Yes (RHP)
13	7745	ZNF192	Zinc finger protein 192	A Kruppel family zinc finger transcription factor	21	11	13, 14	5.12927	Unknown
14	85480	TSLP	Thymic stromal lymphopoietin	A haemopoietic cytokine that enhances the maturation of dendritic cells	21	10	19, 20	4.92555	Yes (RHP)
15	51202	DDX47	DEAD (Asp-Glu-Ala-Asp) box polypeptide 47	A member of the DEAD box protein family RNA helicases	2	11	11, 12	4.90132	Yes (MY)
16	57787	MARK4	MAP/microtubule affinity-regulating kinase 4	A serine/threonine kinase that regulates microtubule organization in neuronal cells	12	13	5, 6	4.38333	Yes (TH)
17	79797	ZNF408	Zinc finger protein 408	A zinc finger protein with the SFP1 domain acting as a transcriptional repressor that regulates cell cycle	21	11	19, 20	4.27504	Unknown

18	9519	TBPL1	TBP-like 1	A general transcription factor that regulates spermatogenesis	3	12	1, 2	4.16447	Yes (OLF)
19	29777	ABT1	Activator of basal transcription 1	A basal transcriptional activator	36	9	15, 16	3.97136	Yes (OLF)
20	6171	RPL41	Ribosomal protein L41	A componet of the 60S ribosome subunit	14	10	7, 8	3.9388	Unknown
21	283337	ZNF740	Zinc finger protein 740	A zinc finger protein of unknown function	20	9	15, 16	3.88503	Unknown
22	51503	CWC15	CWC15 homolog (S. cerevisiae)	A cell cycle control protein involved in mRNA splicing	19	7	13, 14	3.78582	Unknown
23	2273	FHL1	Four and a half LIM domain 1	A protein with the LIM domain that regulates skeletal muscle differentiation	26	3	11, 12	3.75175	Yes (sAMY)
24	65062	ALS2CR4	Amyotrophic lateral sclerosis 2 (juvenile) chromosome region, candidate 4	A membrane protein of unknown function	34	7	7, 8	3.69722	Yes (RHP)
25	8870	IER3	Immediate early response 3	The immediate early gene acting as an antiapoptosis regulator	26	10	13, 14	3.6018	Yes (CB)
26	57179	KIAA1191	KIAA1191	A cytoplasmic protein of unknown function	10	10	13, 14	3.56924	Unknown
27	138428	PTRH1	Peptidyl-tRNA hydrolase 1 homolog (S. cerevisiae)	A peptidyl-tRNA hydrolase	47	10	19, 20	3.55258	Yes (CTX)
28	9659	PDE4DIP	Phosphodiesterase 4D interacting protein (myomegalin)	A protein of the golgi/centrosome that interacts with a cyclic nucleotide phosphodiesterase	25	11	1, 2	3.54046	Yes (HIP)
29	55843	ARHGAP15	Rho GTPase activating protein 15	A Rho GTPase-activating protein acting as a regulator of RAC1	9	6	13, 14	3.50411	Yes (CTX)
30	92170	MTG1	Mitochondrial GTPase 1 homolog (S. cerevisiae)	A mitochondrial GTPase	48	14	7, 8	3.49729	Yes (HIP)
31	84916	CIRH1A	Cirrhosis, autosomal recessive 1 A (cirhin)	A mitochondrial protein with WD40 repeats of unknown function	14	10	19, 20	3.4511	Yes (HIP)
32	26523	EIF2C1	Eukaryotic translation initiation factor 2C, 1	A member of the Argonaute family (AGO1) that plays a role in siRNA-mediated gene silencing	18	11	11, 12	3.43671	Yes (HIP)
33	11091	WDR5	WD repeat domain 5	A protein with WD40 repeats that constitutes a component of histone methyltransferase complexes	20	7	9, 10	3.37083	Yes (HIP)
34	55803	CENTA2	Centaurin, alpha 2	A plasma membrane GTPase activating protein with PH domains	47	12	5, 6	3.25269	Yes (MY)
35	94274	PPP1R14 A	Protein phosphatase 1, regulatory (inhibitor) subunit 14 A	A phosphorylation-dependent inhibitor of smooth muscle myosin phosphatase	9	5	3, 4	3.25117	Yes (MY)
36	1153	CIRBP	Cold-inducible RNA binding protein	A cold stress-inducible protein wuth the RNA recognition motif that plays a role in cold-induced suppression of cell proliferation	16	10	3, 4	3.22391	Yes (CTX)

© 2008 Blackwell Publishing Ltd,

Table 1. (*Continued*)

No.	*Entrez gene ID*	*Gene symbol*	*Gene name*	*Putative molecular function*	*Block*	*Row*	*Column*	*Z-score*	*Gene expression in adult mouse brain (region with the highest expression level)*
37	57732	ZFYVE28	Zinc finger, FYVE domain containing 28	An endosomal protein with the FYVE domain that targets proteins to membrane lipids via interaction with PI3P	12	10	11,12	3.20574	Yes (CB and other regions)
38	84305	WIBG	Within bgcn homolog (Drosophila)	A protein with the Mogo-bind domain of unknown function	43	9	15,16	3.19741	Yes (OLF)
39	55651	NOLA2	Nucleolar protein family A, member 2 (H/ACA small nucleolar RNPs)	A member of the H/ACA snoRNPs gene family that regulates rRNA processing and modification	15	6	15,16	3.155	Yes (OLF)
40	8495	PPFIBP2	PTPRF interacting protein, binding protein 2 (liprin beta 2)	A protein with SAM domains acting as a scaffold for recruitment and anchoring of LAR family PTPases	47	12	11,12	3.13682	Yes (MY)
41	286301	FAM27E3	Family with sequence similarity 27, member E3	A protein of unknown function	14	11	9,10	3.11032	Unknown
42	2258	FGF13	Fibroblast growth factor 13	A member of the FGF family that plays a role in neuronal development	35	11	17,18	3.1035	Yes (HIP)
43	150209	AIFM3	Apoptosis-inducing factor, mitochondrion-associated, 3	A mitochondrial protein with the Rieske domain and the pyridine nucleotide-disulphide oxidoreductase domain acting as an apoptosis inducer	42	10	15,16	3.09063	Unkown
44	1267	CNP	2′,3′-cyclic nucleotide 3′ phosphodiesterase	A cyclic nucleotide phosphodiesterase serving as a marker of myelin	20	10	19,20	3.07624	Yes (CB and other regions)
45	28987	NOB1	NIN1/RPN12 binding protein 1 homolog (S. cerevisiae)	A protein with the PUN domain and the zinc ribbon domain acting as a ribonuclease	14	11	17,18	3.06336	Yes (CB and other regions)
46	55599	RNPC3	RNA-binding region (RNP1, RRM) containing 3	A nuclear protein with RNA recognition motifs that constitutes a component of the U12-type spliceosome	9	8	19,20	3.01035	Yes (OLF)
47	8444	DYRK3	Dual-specificity tyrosine-(Y)-phosphorylation regulated kinase 3	A DYRK family dual-specificity protein kinase that regulates caveolae trafficking	20	13	9,10	3.00278	Yes (HIP)

Among 5000 proteins on the microarray, 47 were identified as the proteins showing a significant interaction. They are listed with Entrez Gene ID, gene symbol, gene name, molecular function, the position on the array, the Z-score and the information on gene expression in the adult mouse brain, including the region with the highest expression level on the sagittal plane of the Allen Brain Atlas.

CB, cerebellum; CTX, cerebral cortex; HIP, hippocampal region; MY, medulla oblongata; OLF, olfactory bulb; sAMY, striatum-like amygdalar nuclei; TH, thalamus; RHP, retrohippocampal region.

© 2008 Blackwell Publishing Ltd,

12 genes in the adult mouse brain is currently unknown. Thus, the expression of PrPIPs is enriched in the adult mouse brain, suggesting the possible interaction of these with PrPC that is expressed broadly at high levels in neurones of the adult rodent CNS [3]. The BIND database search indicated that none of 47 PrPIPs were classified into previously reported PrPC-interacting partners.

We did not detect any negative control spots as positive, including those of BSA, calmodulin, GST, a rabbit anti-GST antibody, human IgG subclasses, an antibiotin antibody and buffer-only control, whereas we identified a battery of positive control spots as positive, such as those of an Alexa Fluor 647-labelled antibody, a biotinylated anti-mouse antibody binding to Alexa Fluor 647-conjugated anti-V5 antibody and V5 protein (Figure 1, panels b–f). The protein microarray we utilized includes only three previously reported PrPC-binding partners, such as glial fibrillary acidic protein [15], tubulin [25] and casein kinase 2 [27] (see Table S2). However, we could not identify them as a significant PrPC interactor in the present study.

Human neurones in culture expressed mRNA of PrPC interactors

Because PrPC *in vivo* is expressed at the highest level in neurones in the CNS, it is important to identify the cell types expressing PrPIPs. By reverse transcription (RT)-PCR analysis, the transcripts coding for PRNP and PR209-interacting proteins, such as FAM64A, PLK3 and MPG, were expressed widely in various human neural and non-neural cell lines (Figure 2, panels a, c, d, e, lanes 3–12). They include cultured human AS, NP cells, NTera2 teratocarcinoma-derived differentiated neurones (NTera2N), Y79 retinoblastoma, SK-N-SH neuroblastoma, IMR-32 neuroblastoma, U-373MG astrocytoma, HMO6 microglia, HeLa cervical carcinoma and HepG2 hepatocellular carcinoma cells. In contrast, high levels of HOXA1 mRNA were expressed in limited cell types, such as NTera2N, U-373MG, HeLa and HepG2 (Figure 2, panel b, lanes 3–12). High levels of PLK3, MPG and PRNP mRNAs were also identified in the human cerebral cortex (CBR) (Figure 2, panels c, d, e, lane 1). The levels of G3PDH mRNA were constant among the cells and tissues examined (Figure 2, panel f, lanes 1, 3–12). By contrast, no products were amplified, when total RNA was processed for PCR without inclusion of the RT step, excluding a contamination of genomic DNA (Figure 2, panels a–f,

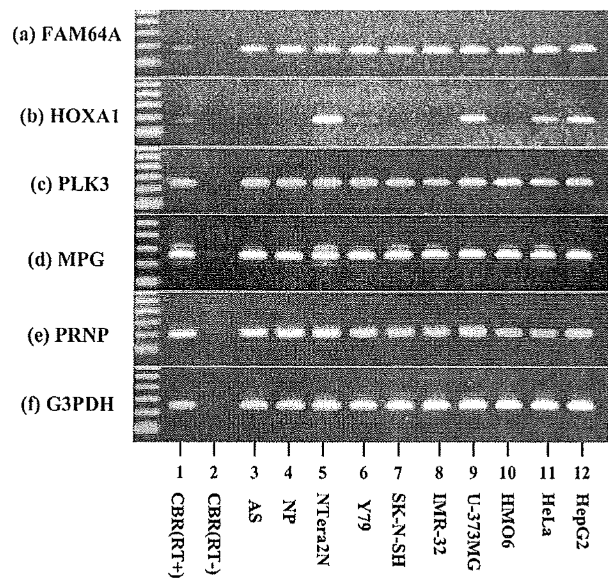

Figure 2. Expression of mRNAs of PrPC interactors in human neural cells. The expression of (a) FAM64A, (b) HOXA1, (c) PLK3, (d) MPG, (e) PRNP and (f) G3PDH mRNAs was studied in human neural and non-neural cells by RT-PCR. The lanes (1–12) represent: (1) the frontal cerebral cortex (CBR) with inclusion of the reverse transcription step (RT+), (2) CBR without inclusion of the reverse transcription step (RT–), (3) cultured astrocytes (AS), (4) cultured neuronal progenitor (NP) cells, (5) NTera2 teratocarcinoma-derived differentiated neurones (NTera2N), (6) Y79 retinoblastoma, (7) SK-N-SH neuroblastoma, (8) IMR-32 neuroblastoma, (9) U-373MG astrocytoma, (10) HMO6 microglia cell line, (11) HeLa cervical carcinoma and (12) HepG2 hepatocellular carcinoma. The DNA size marker (100-bp ladder) is shown on the left.

lane 2). Because NTera2N cells serve as a model of differentiated human neurones in culture [45], these observations suggest that FAM64A, HOXA1, PLK3 and MPG are neuronal proteins coexpressed with PrPC.

Validation of protein microarray data

To verify the results of protein microarray analysis, PR209 and interactors were cloned individually into distinct expression vectors, and were coexpressed transiently in HEK293 cells. FAM64A, HOXA1, PLK3 and MPG were selected for the interactors examined, because of their possible involvement in neural function (see *Discussion*). Because the antibodies suitable for immunoprecipitation with FAM64A, PLK3 and MPG are currently unavailable, we performed immunoprecipitation analysis by using the tag-specific antibodies. First, PR209 was expressed as a Flag-tagged fusion protein, whereas the interactors were

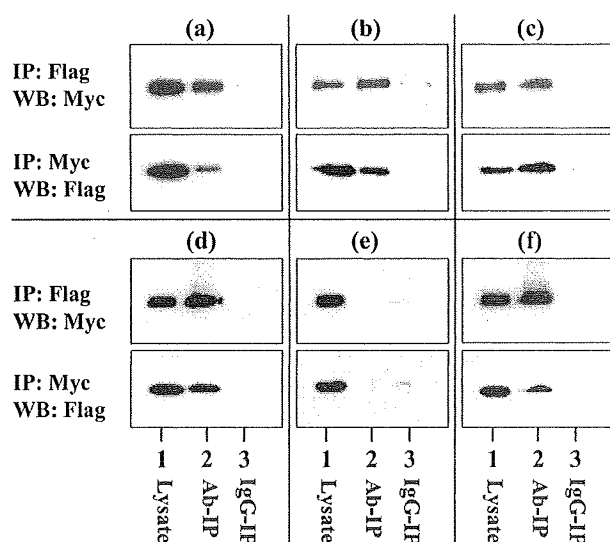

Figure 3. Coimmunoprecipitation analysis. PR209, the N-terminal (NT) half, and the C-terminal (CT) half were expressed as a Flag-tagged fusion protein, while FAM64A, HOXA1, PLK3 and MPG were expressed as a Myc-tagged fusion protein in HEK293 cells. Immunoprecipitation (IP) followed by Western blotting (WB) was performed by using the antibodies against Flag and Myc. The interaction indicates (a) PR209-FAM64A, (b) PR209-PLK3, (c) PR209-MPG, (d) PR209-HOXA1, (e) NT-HOXA1 and (f) CT-HOXA1. The lanes (1–3) represent: (1) input control of cell lysate, (2) IP with anti-Flag or anti-Myc antibody and (3) IP with normal mouse or rabbit IgG.

expressed as a Myc-tagged fusion protein. Coimmunoprecipitation and Western blot validated the interaction of PR209 with FAM64A (Figure 3**a**), PLK3 (Figure 3**b**), MPG (Figure 3**c**) and HOXA1 (Figure 3**d**). Furthermore, we found that not the N-terminal half but the C-terminal half of PR209 is bound to HOXA1 (Figure 3**e**,**f**), excluding non-specific coimmunoprecipitation of PR209 and the interactors in the transient expression system using HEK293 cells.

Next, PR209 was expressed as a DsRed-tagged fusion protein in HEK293 cells. It was located predominantly in the nucleus and the cytoplasm, and less abundantly on the plasma membrane (Figure 4, panels a, d, g, j, m). The EYFP-tagged fusion protein of FAM64A or HOXA1 was located predominantly in the nucleus, where it was colocalized with PR209 (Figure 4, panels b, c, h, i). The EYFP-tagged FAM64A protein was also located chiefly in the nucleus colocalized with DsRed-tagged PR209 in SK-N-SH cells similarly in HEK293, suggesting that the unique subcellular location of FAM64A and PR209 is not attributable to HEK293 cell-specific intracellular trafficking of the recombinant proteins (Figure 4, panels d–f). The GFP-tagged PLK3 fusion protein, expressed on the plasma membrane and in the cytoplasm, showed discernible colocalization with PR209 (Figure 4, panels k, l). The GFP-tagged MPG fusion protein was located chiefly in the nucleus, coexisting with PR209 (Figure 4, panels n, o). Thus, a substantial part of PRP209 and interactors are colocalized in specific subcellular compartments in HEK293 and SK-N-SH cells following transient expression.

Proteinase K sensitivity and detergent insolubility of PR209

To study the proteinase K-resistant property of PR209 coexpressed with the interactors in HEK293 cells, cellular protein extract was treated with proteinase K. In some experiments, the cells were exposed to MG-132 in the last 24 h before harvest. Coexpression of PR209 with HOXA1 or FAM64A did not generate proteinase K-resistant products regardless of treatment with MG-132 (Figure 5**a**, lanes 1–6; upper panel: HOXA1; lower panel: FAM64A). To determine the detergent-insoluble property of PR209, cellular protein extract was separated into 0.5% Nonidet P-40-soluble (S) and -insoluble (P) fractions. Unexpectedly, a great amount of the PR209 protein was recovered from the detergent-insoluble (P) fraction, even when PR209 alone without interactors was transiently expressed in HEK293 cells (Figure 5**b**, lanes 7, 8; upper panel: HOXA1; lower panel: FAM64A). The detergent-insoluble property of PR209 was not affected by coexpression of the interactors, such as HOXA1 or FAM64A, either in the presence or absence of MG-132 (Figure 5, lanes 9–12; upper panel: HOXA1; lower panel: FAM64A). Thus, coexpression of PR209 with the interactors did not produce proteinase K-resistant proteins, although PR209 showed an intrinsic detergent insolubility in HEK293 cells.

Molecular network analysis of PrPC interactors

Functional annotation based on DAVID showed that the great majority of PrPIPs identified by protein microarray analysis play a role in the recognition of nucleic acids, involved in regulation of diverse cellular function (Figure 6).

To identify the molecular network of PrPC and PrPIPs, we imported the list of Entrez gene IDs of 47 PrPIPs into KeyMolnet, the comprehensive biological information

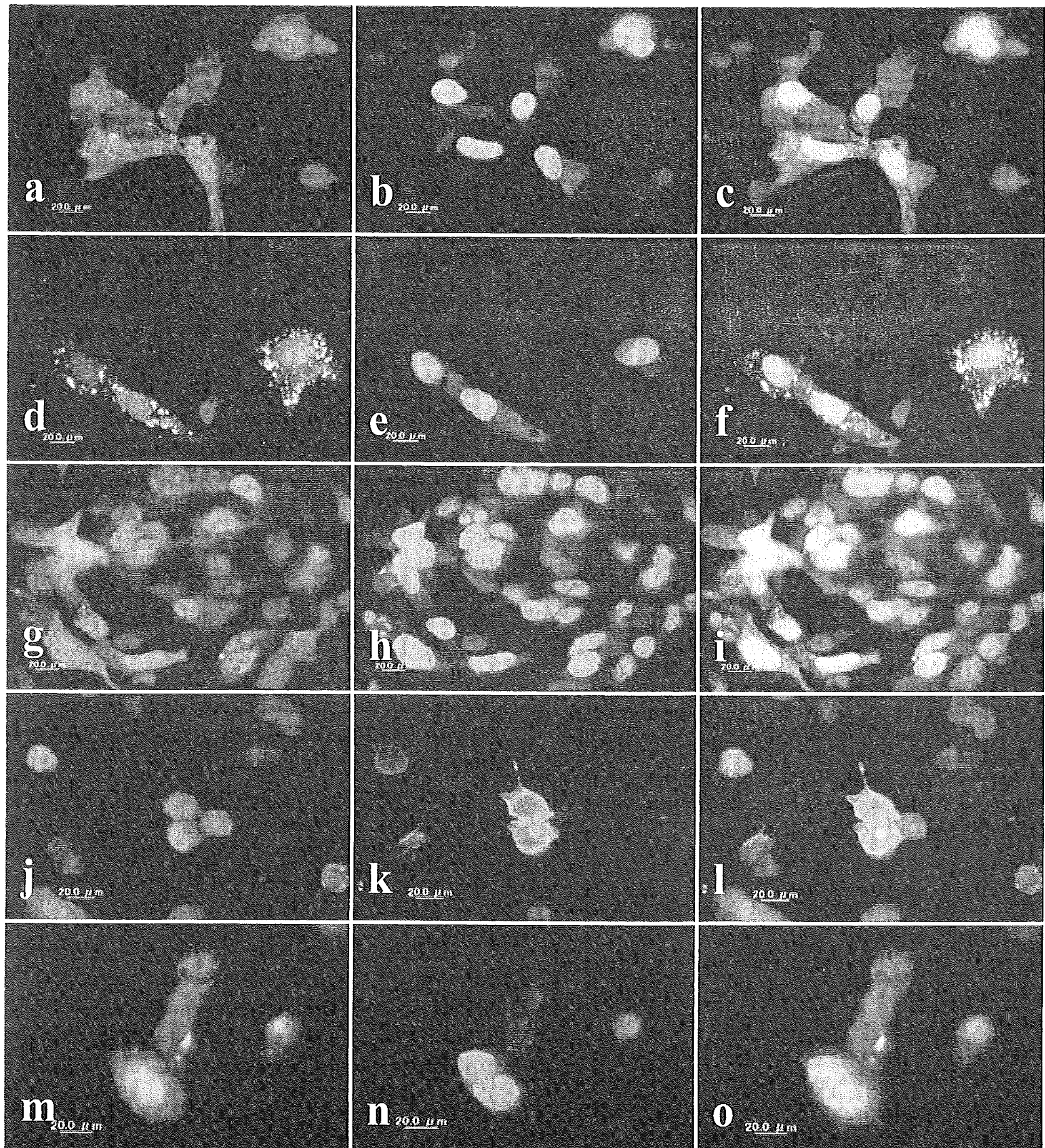

Figure 4. Cell imaging analysis. PR209 was expressed as a DsRed-tagged fusion protein, while FAM64A, HOXA1, PLK3 and MPG were expressed as an EYFP- or GFP-tagged fusion protein in HEK293 cells or in SK-N-SH cells. The panels (a–o) represent (a–c and g–o) HEK293 and (d–f) SK-N-SH of the following: (a) PR209, (b) FAM64A, (c) merge of a and b, (d) PR209, (e) FAM64A, (f) merge of d and e, (g) PR209, (h) HOXA1, (i) merge of g and h, (j) PR209, (k) PLK3, (l) merge of j and k, (m) PR209, (n) MPG and (o) merge of m and n.

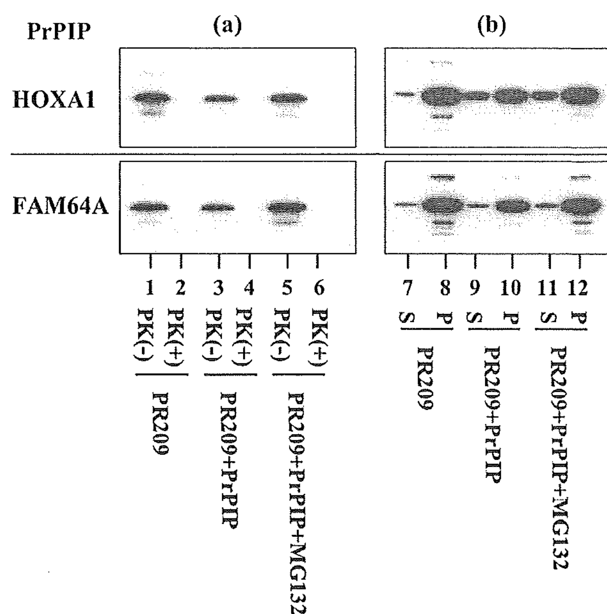

Figure 5. Biochemical property of PR209. Either Flag-tagged PR209 alone (lanes 1, 2, 7, 8) or the combination of PR209 and Myc-tagged PrPIP (lanes 3–6 and 9–12), such as HOXA1 (upper panels) or FAM64A (lower panels), were expressed in HEK293 cells. The cells were harvested at 48 h after transfection of the vectors. In some cultures, the cells were exposed to 10 μM MG-132 during the last 24 h before harvest (lanes 5, 6, 11, 12). (a) Proteinase K treatment. Total cellular protein extract was treated with (+: lanes 2, 4, 6) or without (–: lanes 1, 3, 5) 5 μg/ml proteinase K (PK) at 37°C for 30 min, and then processed for Western blot using 3F4 antibody. (b) Detergent treatment. Total cellular protein extract was separated into 0.5% Nonidet P-40-soluble (S: 50 μg of protein) and -insoluble (P: 7 μg of protein) fractions, and then processed for Western blot using 3F4 antibody.

platform of human molecules and molecular relations. It extracted 39 genes directly linked to 47 PrPIPs. Subsequently, the 'N-points to N-points' search starting from PrPC ending with 39 genes via the shortest route connecting them was performed. This generated a complex molecular network composed of 214 fundamental nodes and 579 molecular relations (Figure 7). Not surprisingly, KeyMolnet operating on the knowledgebase could not identify the direct interaction between PrPC and 47 PrPIPs, because their relationship has not been reported previously. Furthermore, KeyMolnet indicated the primary location of PrPC on the cell-surface membrane, but neither in the cytoplasm nor in the nucleus. When compared with the canonical pathways of KeyMolnet, statistical analysis indicated that the generated network has the most significant relationship with the AKT signalling pathway (the score 50.9). This was followed by the JNK signalling pathway in the second rank (the score 48.4), the MAPK signalling pathway in the third rank (the score 42.8) and the p38 signalling pathway in the fourth rank (the score 36.3). Thus, the molecular network of PrPC and interactors constitutes the key signal-transducing pathways pivotal for regulation of cell differentiation, proliferation, survival and apoptosis.

Discussion

We have performed screening of PrPIPs by using a human protein microarray containing 5000 proteins of various functional classes. By probing the array with PR209 spanning amino acid residues 23–231 of PrPC, we identified 47 novel PrPIPs. The functional annotation on the DAVID database suggested that the great majority of PrPIPs are categorized into the proteins involved in recognition of nucleic acids. The Allen Brain Atlas database search suggested that the great majority of 47 PrPIP orthologues are expressed in the adult rodent brain. Because high-throughput screening of high-density protein microarray enables us to identify a large number of putative binding partners at one time, it is often difficult to extract biological implications of their molecular relationship from such a large quantity of available data. To overcome this difficulty, we have made a breakthrough to identify the molecular network most closely associated with PrPC and the interactors by KeyMolnet, a bioinformatics tool for analysing molecular interaction on the curated knowledge database. The molecular network of PrPC and 47 PrPIPs on KeyMolnet showed an association most relevant to AKT, JNK and MAPK signalling pathways.

Advantages and limitations of protein microarray technology for identification of protein–protein interaction

Protein microarray serves as a powerful tool for the rapid and systematic identification of protein–protein and other biomolecule interactions. Protein microarray has a wide range of applications, including characterization of antibody specificity and autoantibody repertoire, and identification of novel biomarkers and molecular targets associated with disease type, stage and progression, leading to establishment of personalized medicine [47–49].

However, protein microarray technology is still under development in methodological aspects. In general,

© 2008 Blackwell Publishing Ltd,

Category	Term	RT	Genes	Count	%	P-Value
SP_PIR_KEYWORDS	rna-binding	RT		5	10.6	4.5E-3
SP_PIR_KEYWORDS	nuclear protein	RT		12	25.5	7.7E-3
GOTERM_CC_ALL	nucleus	RT		14	29.8	1.4E-2
INTERPRO_NAME	Nucleotide-binding, alpha-beta plait	RT		4	8.5	1.4E-2
GOTERM_MF_ALL	nucleic acid binding	RT		14	29.8	1.6E-2
SP_PIR_KEYWORDS	zinc-finger	RT		7	14.9	2.9E-2
GOTERM_MF_ALL	molecular function unknown	RT		5	10.6	4.4E-2
GOTERM_CC_ALL	intracellular organelle	RT		18	38.3	5.6E-2
GOTERM_CC_ALL	organelle	RT		18	38.3	5.6E-2
GOTERM_MF_ALL	nucleotide binding	RT		9	19.1	5.8E-2
SP_PIR_KEYWORDS	ribonucleoprotein	RT		3	6.4	5.9E-2
SP_PIR_KEYWORDS	alternative splicing	RT		11	23.4	6.1E-2
GOTERM_MF_ALL	RNA polymerase II transcription factor activity	RT		3	6.4	6.7E-2
SP_PIR_KEYWORDS	zinc	RT		7	14.9	6.8E-2
GOTERM_BP_ALL	nucleobase, nucleoside, nucleotide and nucleic acid metabolism	RT		11	23.4	7.4E-2
GOTERM_CC_ALL	intracellular	RT		20	42.6	7.5E-2
INTERPRO_NAME	RNA-binding region RNP-1 (RNA recognition motif)	RT		3	6.4	7.8E-2
GOTERM_BP_ALL	cellular metabolism	RT		19	40.4	7.9E-2
SMART_NAME	RRM	RT		3	6.4	8.2E-2
UP_SEQ_FEATURE	splice variant	RT		11	23.4	8.6E-2
GOTERM_CC_ALL	ribonucleoprotein complex	RT		4	8.5	8.7E-2
UP_SEQ_FEATURE	zinc finger region:C4-type	RT		2	4.3	9.0E-2
SP_PIR_KEYWORDS	dna-binding	RT		6	12.8	9.5E-2
GOTERM_BP_ALL	development	RT		7	14.9	9.6E-2

Figure 6. Functional annotation of PrPC interactors. Functional annotation of 47 PrPIPs identified by protein microarray analysis was performed by the program on DAVID bioinformatics database. When the list of Entrez gene IDs of 47 PrPIPs was imported, 34 genes were functionally categorized into 24 subgroups created by related databases, with enriched terms closely associated with the gene list examined. The genes excluded from the list ($n = 13$) are FAM64A, C7orf50, SCNM1, C18orf56, DKFZp761B107, TSLP, CWC15, KIAA1191, ARHGAP15, WDR5, WIBG, FAM27E3 and NOB1 (see Table 1 for the gene symbol). RT represents related term search. Genes and count indicate the genes involved in the term. The percentage is calculated from the formula following: gene involvement (%) = involved genes/total genes. *P*-value represents the *P*-value of gene enrichment analysis evaluated by the modified Fisher's exact test where it is the smaller, the genes are the more enriched in the term.

protein microarray has its own limitation associated with the expression and purification of a wide variety of target proteins. In the microarray we utilized, the target proteins were expressed in a baculovirus expression system, purified under native conditions, and spotted on to the slides to ensure the preservation of native structure, post-translational modifications such as glycosylation and phosphorylation [50], and proper functionality. In contrast, bacterially expressed proteins lack glycosylation and phosphorylation moieties, and are often misfolded during purification. As target proteins contain a GST fusion tag, the arrays are always processed for the post-spotting quality control by using an anti-GST antibody with a concentration gradient of GST spots as a standard. This procedure makes it possible to quantify the exact amount of proteins deposited in each spot, and thereby minimizes the inter-lot variability of the results. Furthermore, each sub-array contains a series of built-in control spots.

Protein microarray also has another technical limitation attributable to the avidity of protein–protein interaction. The probing and rigorous washing procedure detects mostly the direct protein–protein interaction supported by the stable binding ability. It could not efficiently detect weak and transient protein–protein interactions, or indirect interactions that require accessory molecules or intervening cofactors. In addition, protein microarray screening does not consider the specific subcellular location where the protein–protein interaction actually takes

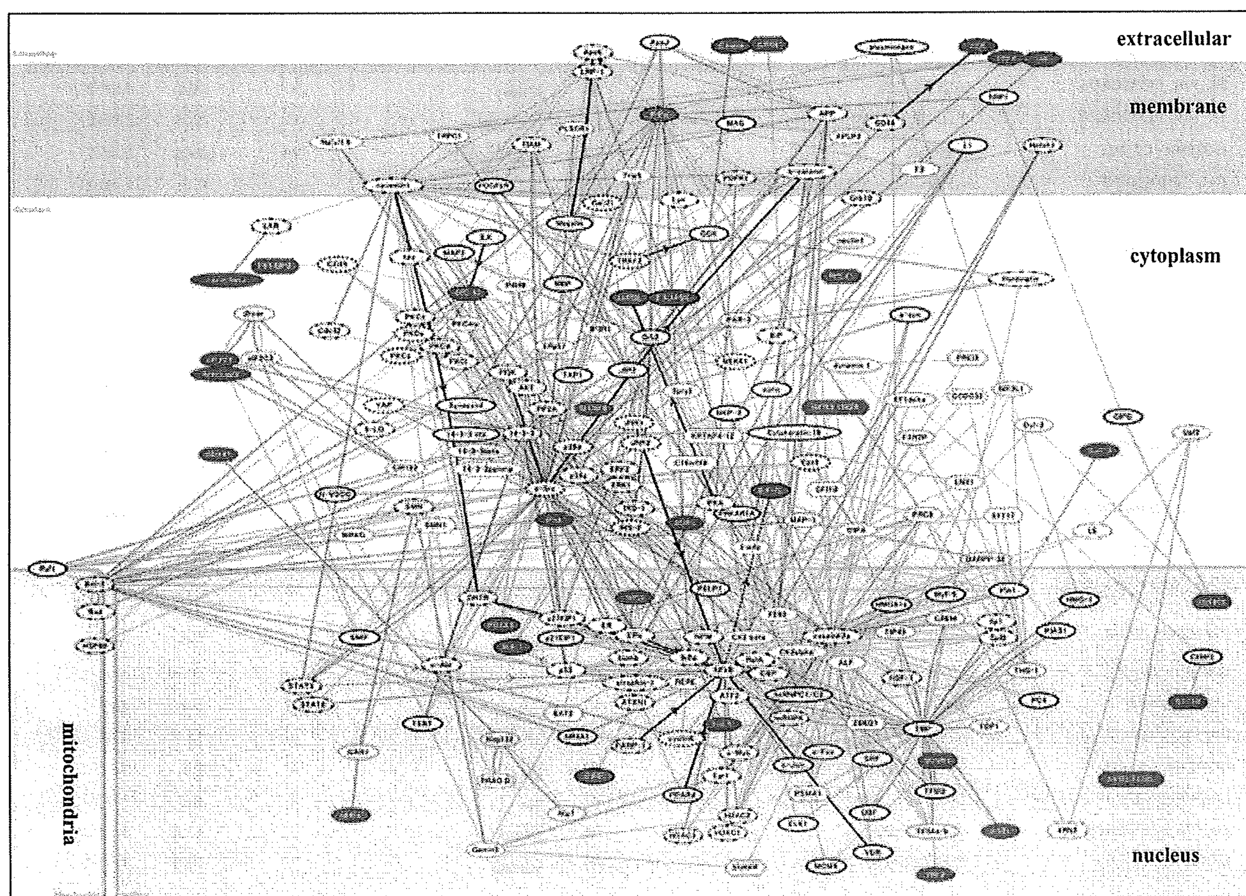

Figure 7. Molecular network of PrPC and the interactors. By importing the list of Entrez gene IDs of 47 PrPIPs, KeyMolnet extracted 39 genes directly linked to 47 PrPIPs. Subsequently, the 'N-points to N-points' search starting from PrPC ending with 39 genes generated a complex molecular network composed of 214 fundamental nodes and 579 molecular relations. They are arranged according to the predicted subcellular location. The red node indicates PrPC on the cell-surface membrane as the starting point, while blue nodes represent PrPIPs listed in Table 1. The connections of thick lines represent the core contents, while thin lines indicate the secondary contents of KeyMolnet. The molecular relation is indicated by dash line with arrow (transcriptional activation), solid line with arrow (direct activation) or solid line without arrow (direct interaction or complex formation).

place. Thus, it is possible that some promiscuous partners are detected, whereas some of the biologically important interactors *in vivo* are left beyond identification. Therefore, protein microarray data always require the validation by other independent methods such as coimmunoprecipitation, far Western blotting, the Y2H screening and so on. Post-translational modifications play a pivotal role in a range of protein–protein interactions. Immunolabelling of the array we utilized with anti-phosphotyrosine antibody showed that approximately 10–20% of the proteins on the array are phosphorylated (Invitrogen, unpubl. data). When the array was utilized for kinase substrate identification, most of known kinases immobilized on the array are enzymatically active with the capacity for autophosphorylation, suggesting that they are functionally active with preservation of proper conformation (data of Invitrogen).

Validation of interaction and colocalization of PrPC with four neuronal PrPC interactors by immunoprecipitation and cell imaging analysis

We selected four PrPIPs for further biochemical characterization, including FAM64A, HOXA1, PLK3 and MPG, because of their potential involvement in neural function. Furthermore, we identified the expression of all of these in differentiated human neurones NTera2N by RT-PCR. FAM64A is a 26-kDa protein with a DUF1466 domain in its N-terminal region. Currently, its biological function

remains unknown. However, the database search on Entrez UniGene, the organized view of the transcriptome, showed that the FAM64A transcript is expressed abundantly in brain tissues, glioma and primitive neuroectodermal tumours. HOXA1 acts as a transcription factor that regulates the proper arrangement of hindbrain segments during development [51]. Homozygous truncating mutations in the human HOXA1 gene disrupt brainstem, inner ear, cardiovascular and cognitive development in patients with the Bosley–Salih–Aloraïny syndrome [52]. PLK3 is a member of the polo family serine/threonine kinases that regulate the onset of mitosis and M-phase progression in cell cycle. Long-term potentiation enhances PLK3 expression in hippocampal neurones, suggesting a role of PLK3 in synaptic plasticity [53]. MPG is a DNA repair enzyme that removes mutagenic alkylation adducts of purines from damaged DNA. Astrocytoma cells express a great amount of MPG protein, supporting a role of MPG in astrocytic tumorigenesis [54].

The interaction of PR209 with FAM64A, HOXA1, PLK3 and MPG was verified by coimmunoprecipitation and cell imaging in a transient expression system of HEK293 cells. Because the antibodies sufficient for immunoprecipitation with FAM64A, PLK3 and MPG are currently unavailable, we performed immunoprecipitation analysis by using the tag-specific antibodies. Although cultured human neurones, such as NTera2, appear to be preferable for expression of PrPC interactors, we utilized HEK293 cells because of much easier handling and constant expression of tagged recombinant proteins. It is worth noting that in preliminary experiments, we found that there exists a small but discernible level of interaction between endogeneous PrPC and HOXA1 in adult human brain tissue homogenates (data not shown).

PrPC is structurally separated into two distinct segments composed of the N-terminal flexibly disordered tail (amino acid residues 23–121) that includes the octapeptide repeat region, and the C-terminal globular domain (amino acid residues 121–230) that contains three α-helices and two short anti-parallel β-sheets [55]. The immunoprecipitation study showed that HOXA1 interacts exclusively with the C-terminal half of PR209.

PrPC interactors play a role in nuclear function

Although PrPC is a glycosylphosphatidylinositol (GPI)-anchored cell-surface protein, we found that DsRed-tagged PR209 with the C-terminal GPI anchor site of amino acid residue 231 is located predominantly in the nucleus and the cytoplasm, and less abundantly on the plasma membrane. A recent study showed that PrPC after cleavage of both N-terminal and C-terminal signal peptides is located chiefly in the nucleus, where it interacts with chromatin in neural cell lines [56], supporting our findings that PrPC could interact with its partners in both the nucleus and the cytoplasm. PrPC has two cryptic nuclear localization signals in the N-terminal domain [57]. Nuclear localization of PrPSc-like protein is identified in prion-infected cells [58]. Furthermore, defined populations of neurones express PrPC in their cytoplasm [59]. In the present study, FAM64A, HOXA1 and MPG were located predominantly in the nucleus, where they coexisted with PR209. The involvement of PrPC and interactors in nuclear function is supported by functional annotation on the DAVID database that suggested a major role of PrPIPs in the recognition of nucleic acids. We could categorize the nucleic acid-binding PrPIPs into two distinct groups: (i) proteins involved in RNA splicing, silencing and metabolism: SCNM1, RBM22, DDX47, CWC15, PTRH1, EIF2C1, CIRBP, NOLA2, NOB1 and RNPC3, and (ii) proteins involved in DNA transcription and repair: HOXA1, BAZE2B, MPG, ZNF192, ZNF408, TBPL1, ABT1, ZNF740 and WDR5. Importantly, a previous study indicated that PrPC plays a key role in nucleic acid metabolism by its nucleic acid chaperoning activity [60]. Because protein microarray analysis utilized the recombinant PR209 highly purified from the culture supernatant as a probe, the possibility is unlikely that any contaminating cellular nucleic acids mediate the interaction between PrPC and PrPIPs.

Previous studies showed that PrPC spanning amino acid residues 23–230 designated CyPrP accumulates in the cytoplasm, where it is converted into the PrPSc-like proteinase K-resistant protein (PrP^{RES}) with potent neurotoxicity, when the proteasome activity is suppressed [61,62]. In contrast, we showed that coexpression of large amounts of PR209 with HOXA1 or FAM64A did not generate PrP^{RES} in HEK293 cells, even after exposure of the cells to MG-132. Our observations suggest that both HOXA1 and FAM64A do not act as the chaperone 'protein X' that promotes protein conformational conversion from PrPC to PrPSc at least in a short incubation time of 48 h. Because prion diseases develop after a long incubation period, our observations do not exclude the possibility that a long-term incubation of PrPC and the interactors with some additional cofactors could accelerate the conforma-

tional conversion from PrPC to PrPSc. In addition, we unexpectedly found that PR209 exhibits an intrinsic detergent insolubility in HEK293 cells following transient overexpression. A recent study showed that small amounts of detergent-insoluble prion protein aggregates are present in normal human brains [63].

The molecular network of PrPC and interactors involves key cell signalling pathways

KeyMolnet stores the comprehensive content database that focuses on human molecules and molecular interactions, carefully curated by experts from the literature and public databases [41]. This software makes it possible to effectively extract the most relevant molecular interaction from large quantities of gene expression data, and to establish a biologically relevant logical working model [42]. The present study for the first time by using KeyMolnet, a data-mining tool of bioinformatics, showed that the complex molecular network of PrPC and 47 PrPIPs has a significant relationship with AKT, JNK and MAPK signalling pathways. A previous study showed that PrPC activates diverse signalling pathways involving Fyn, PI3 kinase/Akt, cAMP-dependent protein kinase A and MAP kinase, all of which contribute to neurite outgrowth and neuronal survival in primary culture of mouse neurones [64]. PrPC-knockout mice show exacerbation of ischaemic brain injury, accompanied by reduced expression of Ser473-phosphorylated Akt and increased activities of ERK-1/-2, STAT-1 and caspase-3 in the brain [65,66]. A synthetic peptide PrP106–126 induces neuronal apoptosis in primary cultures of mouse neurones via the JNK-c-Jun pathway [67]. All of these observations suggest a crucial link between the biological function of PrPC and signalling pathways mediated by AKT, JNK and MAPK.

Previously, we showed that the genes located in the Ras/Rac signalling pathway, pivotal for cell proliferation, differentiation and survival, were aberrantly regulated in cultured fibroblasts of PrPC-deficient mice [68]. More recently, by analysing a DNA microarray containing 12 814 human genes, we identified 33 genes differentially expressed between a stable PrPC-expressing HEK293 cell line and the parent PrPC-non-expressing cells [37]. They included 18 genes involved in neuronal and glial functions, five related to production of the extracellular matrix, and two located in the complement cascade. These observations suggest that aberrant expression of PrPC, either overexpression or underexpression, affects a wide range of cell signalling pathways. Most recently, we showed that the zeta isoform of 14-3-3 protein, a scaffold protein on which diverse signal components converge, forms a molecular complex with PrPC and heat shock protein Hsp60 in the human CNS neurones under physiological conditions [23]. This raises the hypothesis that the multimolecular complex is disrupted in the pathological process of prion diseases, resulting in the release of 14-3-3 from degenerating neurones into the cerebrospinal fluid. Unfortunately, the protein microarray utilized in the present study does not include 14-3-3 zeta, Hsp60 or PrPC as targets.

In conclusion, protein microarray is a useful tool for systematic screening and comprehensive profiling of the human PrPC interactome. The great majority of PrPIPs are annotated as the proteins involved in the recognition of nucleic acids. Thus, individual PrPIPs possibly act as regulators of RNA splicing, silencing, and metabolism and modulators for DNA transcription and repair in neural and non-neural cells. Furthermore, the human PrPC–PrPIP network on the whole plays a pivotal role in signalling pathways essential for regulation of cell survival, differentiation, proliferation and apoptosis. These observations propose a logical hypothesis that the dysregultion of PrPC interactome might induce extensive neurodegeneration ongoing in prion diseases, and warrant further studies to clarify the implication of PrPC and the interactors in cellular signalling and nuclear function.

Acknowledgements

This work was supported by the Grant-in-Aid for Scientific Research, the Ministry of Education, Culture, Sports, Science and Technology, Japan (B18300118), the grants from Research on Psychiatric and Neurological Diseases and Mental Health, the Ministry of Health, Labour and Welfare of Japan (H17-020) and Research on Health Sciences Focusing on Drug Innovation, the Japan Health Sciences Foundation (KH21101), and the Nakatomi Foundation.

References

1 Prusiner SB. Prions. *Proc Natl Acad Sci USA* 1998; **95**: 13363–83

2 Aguzzi A, Polymenidou M. Mammalian prion biology: one century of evolving concepts. *Cell* 2004; **116**: 313–27

3 Bendheim PE, Brown HR, Rudelli RD, Scala LJ, Goller NL, Wen GY, Kascsak RJ, Cashman NR, Bolton DC. Nearly ubiquitous tissue distribution of the scrapie agent precursor protein. *Neurology* 1992; **42**: 149–56
4 Telling GC, Scott M, Mastrianni J, Gabizon R, Torchia M, Cohen FE, DeArmond SJ, Prusiner SB. Prion propagation in mice expressing human and chimeric PrP transgenes implicates the interaction of cellular PrP with another protein. *Cell* 1995; **83**: 79–90
5 Kaneko K, Zulianello L, Scott M, Cooper CM, Wallace AC, James TL, Chen FE, Prusiner SB. Evidence for protein X binding to a discontinuous epitope on the cellular prion protein during scrapie prion propagation. *Proc Natl Acad Sci USA* 1997; **94**: 10069–74
6 Büeler H, Fischer M, Lang Y, Bluethmann H, Lipp HP, DeArmond SJ, Prusiner SB, Aguet M, Weissmann C. Normal development and behaviour of mice lacking the neuronal cell-surface PrP protein. *Nature* 1992; **356**: 577–82
7 Manson JC, Clarke AR, Hooper ML, Aitchison L, McConnell I, Hope J. 129/Ola mice carrying a null mutation in PrP that abolishes mRNA production are developmentally normal. *Mol Neurobiol* 1994; **8**: 121–7
8 Sakaguchi S, Katamine S, Nishida N, Moriuchi R, Shigematsu K, Sugimoto T, Nakatani A, Kataoka Y, Houtani T, Shirabe S, Okada H, Hasegawa S, Miyamoto T, Noda T. Loss of cerebellar Purkinje cells in aged mice homozygous for a disrupted PrP gene. *Nature* 1996; **380**: 528–31
9 Graner E, Mercadante AF, Zanata SM, Forlenza OV, Cabral ALB, Veiga SS, Juliano MA, Roesler R, Walz R, Minetti A, Izquierdo I, Martins VR, Brentani RR. Cellular prion protein binds laminin and mediates neuritogenesis. *Mol Brain Res* 2000; **76**: 85–92
10 Lopes MH, Hajj GNM, Muras AG, Mancini GL, Castro RMPS, Ribeiro KCB, Brentani RR, Linden R, Martins VR. Interaction of cellular prion and stress-inducible protein 1 promotes neuritogenesis and neuroprotection by distinct signaling pathways. *J Neurosci* 2005; **25**: 11330–9
11 Schmitt-Ulms G, Legname G, Baldwin MA, Ball HL, Bradon N, Bosque PJ, Crossin KL, Edelman GM, DeArmond SJ, Cohen FE, Prusiner SB. Binding of neural cell adhesion molecules (N-CAMs) to the cellular prion protein. *J Mol Biol* 2001; **314**: 1209–25
12 Chiarini LB, Freitas ARO, Zanata SM, Brentani RR, Martins VR, Linden R. Cellular prion protein transduces neuroprotective signals. *EMBO J* 2002; **21**: 3317–26
13 Brown DR, Qin K, Herms JW, Madlung A, Manson J, Strome R, Fraser PE, Kruck T, von Bohlen A, Schulz-Schaeffer W, Giese A, Westaway D, Kretzschmar H. The cellular prion protein binds copper in vivo. *Nature* 1997; **390**: 684–7
14 Spielhaupter C, Schätzl HM. PrP^{C} directly interacts with proteins involved in signaling pathways. *J Biol Chem* 2001; **276**: 44604–12
15 Oesch B, Teplow DB, Stahl N, Serban D, Hood LE, Prusiner SB. Identification of cellular proteins binding to the scrapie prion protein. *Biochemistry* 1990; **29**: 5848–55
16 Yehiely F, Bamborough P, Da Costa M, Perru BJ, Thinakaran G, Cohen FE, Carlson GA, Prusiner SB. Identification of candidate proteins binding to prion protein. *Neurobiol Dis* 1997; **2**: 339–55
17 Edenhofer F, Rieger R, Famulok M, Wendler W, Weiss S, Winnacker EL. Prion protein PrP^{C} interacts with molecular chaperones of the Hsp60 family. *J Virol* 1996; **70**: 4724–8
18 DebBurman SK, Raymond GJ, Caughey B, Lindquist S. Chaperone-supervised conversion of prion protein to its protease-resistant form. *Proc Natl Acad Sci USA* 1997; **94**: 13938–43
19 Stöckel J, Hartl FU. Chaperonin-mediated de novo generation of prion protein aggregates. *J Mol Biol* 2001; **313**: 861–72
20 Zanata SM, Lopes MH, Mercadante AF, Hajj GN, Chiarini LB, Nomizo R, Freitas AR, Cabral AL, Lee KS, Juliano MA, de Oliveira E, Jachieri SG, Burlingame A, Huang L, Linden R, Brentani RR, Martins VR. Stress-inducible protein 1 is a cell surface ligand for cellular prion that triggers neuroprotection. *EMBO J* 2002; **21**: 3307–16
21 Kurschner C, Morgan JI. Analysis of interaction sites in homo- and heteromeric complexes containing Bcl-2 family members and the cellular prion protein. *Mol Brain Res* 1996; **37**: 249–58
22 Mattei V, Garofalo T, Misasi R, Circella A, Manganelli V, Lucania G, Pavan A, Sorice M. Prion protein is a component of the multimolecular signaling complex involved in T cell activation. *FEBS Lett* 2004; **560**: 14–18
23 Satoh J, Onoue H, Arima K, Yamamura T. The 14-3-3 protein forms a molecular complex with heat shock protein Hsp60 and cellular prion protein. *J Neuropathol Exp Neurol* 2005; **64**: 858–68
24 Bragason BT, Palsdottir A. Interaction of PrP with NRAGE, a protein involved in neuronal apoptosis. *Mol Cell Neurosci* 2005; **29**: 232–44
25 Nieznanski K, Nieznanska H, Skowronek KJ, Osiecka KM, Stepkowski D. Direct interaction between prion protein and tubulin. *Biochem Biophys Res Commun* 2005; **334**: 403–11
26 Strom A, Diecke S, Hunsmann G, Stuke AW. Identification of prion protein binding proteins by combined use of far-western immunoblotting, two dimensional gel electrophoresis and mass spectrometry. *Proteomics* 2006; **6**: 26–34
27 Meggio F, Negro A, Sarno S, Ruzzene M, Bertoli A, Sorgato MC, Pinna LA. Bovine prion protein as a modulator of protein kinase CK2. *Biochem J* 2000; **352**: 191–6
28 Fischner MB, Roeckl C, Parizek P, Schwarz HP, Aguzzi A. Binding of disease-associated prion protein to plasminogen. *Nature* 2000; **408**: 479–83

29 Rieger R, Edenhofer F, Lasmézas CI, Weiss S. The human 37-kDa laminin receptor precursor interacts with the prion protein in eukaryotic cells. *Nat Med* 1997; 3: 1283–8

30 Hajj GN, Lopes MH, Mercadante AF, Veiga SS, da Silveira RB, Santos TG, Ribeiro KC, Juliano MA, Jacchieri SG, Zanata SM, Martins VR. Cellular prion protein interaction with vitronectin supports axonal growth and is compensated by integrins. *J Cell Sci* 2007; **120**: 1915–26

31 von Mering C, Krause R, Snel B, Cornell M, Oliver SG, Fields S, Bork P. Comparative assessment of large-scale data sets of protein–protein interactions. *Nature* 2002; **417**: 399–403

32 Vidalain PO, Boxem M, Ge H, Li S, Vidal M. Increasing specificity in high-throughput yeast two-hybrid experiments. *Methods* 2004; **32**: 363–70

33 MacBeath G, Schreiber SL. Printing proteins as microarrays for high-throughput function determination. *Science* 2000; **289**: 1760–3

34 Chan SM, Ermann J, Su L, Fathman CG, Utz PJ. Protein microarrays for multiplex analysis of signal transduction pathways. *Nat Med* 2004; **10**: 1390–6

35 Schweitzer B, Predki P, Snyder M. Microarrays to characterize protein interactions on a whole-proteome scale. *Proteomics* 2003; **3**: 2190–9

36 Satoh J. Protein microarray analysis for rapid identification of 14-3-3 protein binding partners. In *Functional Protein Microarrays in Drug Discovery*. Ed. Predki PF. Boca Raton: CRC Press, 2007; 239–59

37 Satoh J, Yamamura T. Gene expression profile following stable expression of the cellular prion protein. *Cell Mol Neurobiol* 2004; **24**: 793–814

38 Satoh J, Nanri Y, Yamamura T. Rapid identification of 14-3-3-binding proteins by protein microarray analysis. *J Neurosci Methods* 2006; **152**: 278–88

39 Lein ES, Hawrylycz MJ, Ao N, Ayres M, Bensinger A, Bernard A, Boe AF, Boguski MS, Brockway KS, Byrnes EJ, Chen L, Chen L, Chen TM, Chin MC, Chong J, Crook BE, Czaplinska A, Dang CN, Datta S, Dee NR, Desaki AL, Desta T, Diep E, Dolbeare TA, Donelan MJ, Dong HW, Dougherty JG, Duncan BJ, Ebbert AJ, Eichele G, Estin LK, Faber C, Facer BA, Fields R, Fischer SR, Fliss TP, Frensley C, Gates SN, Glattfelder KJ, Halverson KR, Hart MR, Hohmann JG, Howell MP, Jeung DP, Johnson RA, Karr PT, Kawal R, Kidney JM, Knapik RH, Kuan CL, Lake JH, Laramee AR, Larsen KD, Lau C, Lemon TA, Liang AJ, Liu Y, Luong LT, Michaels J, Morgan JJ, Morgan RJ, Mortrud MT, Mosqueda NF, Ng LL, Ng R, Orta GJ, Overly CC, Pak TH, Parry SE, Pathak SD, Pearson OC, Puchalski RB, Riley ZL, Rockett HR, Rowland SA, Royall JJ, Ruiz MJ, Sarno NR, Schaffnit K, Shapovalova NV, Sivisay T, Slaughterbeck CR, Smith SC, Smith KA, Smith BI, Sodt AJ, Stewart NN, Stumpf KR, Sunkin SM, Sutram M, Tam A, Teemer CD, Thaller C, Thompson CL, Varnam LR, Visel A, Whitlock RM, Wohnoutka PE, Wolkey CK, Wong VY, Wood M, Yaylaoglu MB, Young RC, Youngstrom BL, Yuan XF, Zhang B, Zwingman TA, Jones AR. Genome-wide atlas of gene expression in the adult mouse brain. *Nature* 2007; **445**: 168–76

40 Dennis G Jr, Sherman BT, Hosack DA, Yang J, Gao W, Lane HC, Lempicki RA. DAVID: database for annotation, visualization, and integrated discovery. *Genome Biol* 2003; **4**: R60

41 Sato H, Ishida S, Toda K, Matsuda R, Hayashi Y, Shigetaka M, Fukuda M, Wakamatsu Y, Itai A. New approaches to mechanism analysis for drug discovery using DNA microarray data combined with KeyMolnet. *Curr Drug Discov Technol* 2005; **2**: 89–98

42 Satoh J, Illes Z, Peterfalvi A, Tabunoki H, Rozsa C, Yamamura T. Aberrant transcriptional regulatory network in T cells of multiple sclerosis. *Neurosci Lett* 2007; **422**: 30–3

43 Butler DA, Scott MRD, Bockman JM, Borchelt DR, Taraboulos A, Hsiao KK, Kingsbury DT, Prusiner SB. Scrapie-infected murine neuroblastoma cells produce protease-resistant prion proteins. *J Virol* 1998; **62**: 1558–64

44 Lorenz H, Windl O, Kretzschmar HA. Cellular phenotyping of secretory and nuclear prion proteins associated with inherited prion diseases. *J Biol Chem* 2002; **277**: 8508–16

45 Satoh J, Kuroda Y. Differential gene expression between human neurons and neuronal progenitor cells in culture: an analysis of arrayed cDNA clones in NTera2 human embryonal carcinoma cell line as a model system. *J Neurosci Methods* 2000; **94**: 155–64

46 Vincent B, Paitel E, Saftig P, Frobert Y, Hartmann D, De Strooper B, Grassi J, Lopez-Perez E, Checler F. The disintegrations ADAM10 and TACE contribute to the constitutive and phorbol ester-regulated normal cleavage of the cellular prion protein. *J Biol Chem* 2001; **276**: 37743–6

47 Robinson WH, Fontoura P, Lee BJ, de Vegvar HE, Tom J, Pedotti R, DiGennaro CD, Mitchell DJ, Fong D, Ho PP, Ruiz PJ, Maverakis E, Stevens DB, Bernard CC, Martin R, Kuchroo VK, van Noort JM, Genain CP, Amor S, Olsson T, Utz PJ, Garren H, Steinman L. Protein microarrays guide tolerizing DNA vaccine treatment of autoimmune encephalomyelitis. *Nat Biotechnol* 2003; **21**: 1033–9

48 Quintana FJ, Hagedorn PH, Elizur G, Merbl Y, Domany E, Cohen IR. Functional immunomics: microarray analysis of IgG autoantibody repertoires predicts the future response of mice to induced diabetes. *Proc Natl Acad Sci USA* 2004; **101**: 14615–21

49 Zangar RC, Varnum SM, Bollinger N. Studying cellular processes and detecting disease with protein microarray. *Drug Metab Rev* 2005; **37**: 473–87

50 Tennagels N, Hube-Magg C, Wirth A, Noelle V, Klein HW. Expression, purification, and characterization of the cytoplasmic domain of the human IGF-1 receptor using a baculovirus expression system. *Biochem Biophys Res Commun* 1999; **260**: 724–8

© 2008 Blackwell Publishing Ltd,